Automatic mapping of hydrocarbon pollution based on hyperspectral imaging

Véronique Achard, Christopher Elin

AUTOMATIC MAPPING OF HYDROCARBON POLLUTION BASED ON HYPERSPECTRAL IMAGING

Véronique Achard, Christopher Elin
ONERA, The French Aerospace Lab., 2 av. Edouard Belin, 31055 TOULOUSE

ABSTRACT

Large-scale mapping of coastal oil spills and their monitoring over time is a major issue that can be adressed by using hyperspectral images and dedicated processing. Previous researches have shown that it is possible to map the polluted coastline caused by the explosion of the Deepwater Horizon (DwH) platform from AVIRIS images (AVIRIS: Airborne Visible/InfraRed Imaging Spectrometer). But the detection processes required either ground truth or laboratory spectra of hydrocarbons or were not fully automatic.

In this paper we focused on an AVIRIS image which covers The Bay Jimmy, located south of New Orleans, and particularly impacted by oil pollution. Two automatic methods were developed to detect oiled coasts. In the first one, we have developed a new spectral index able to detect directly hydrocarbon and less sensitive to noise than indices proposed in previous works. The second one extracts endmembers via Orthogonal Subspace Projection, and then sorts the endmembers in terms of hydrocarbon indices scores, in descending order. Then, the detection map or the abundance map corresponding to the best endmember is used to map oiled areas. Both approaches give results consistent with those of studies previously conducted on the same image, and with maps built from field observations.

Index Terms— *Hyperspectral, Oil spill, Automatic Detection, spectral unmixing, hydrocarbon indices*

1. INTRODUCTION

In 2010, the United States suffered the largest oil spill in its history, with a leak of about 4.9 million barrels of oil. An important cleaning effort was done to prevent crude oil from reaching coastline. However, a significant amount of oil spilled over shorelines [1] [2].

As oil was spreading along the Louisiana coasts, hyperspectral images have been acquired with the AVIRIS sensor. Previous studies have shown the potential of using remote sensing to detect oiled coastlines, [3], [4]. Oil detection methods are based on two main hydrocarbon absorption bands at 1.73 µm and 2.3 µm. The difficulty lies in the fact that dry or senescent plants have similar spectral characteristics that can cause false alarms.

To map coastal lines impacted by DWH Oil, Kokaly et al. [3] used the Material Identification and Characterization Algorithm (MICA) of the PRISM module (Processing Routines in IDL for Spectroscopic Measurement) of the USGS (United States Geological Survey) [5]. It compares the spectrum of each pixel with reference spectra obtained either by field or lab measurements. Another method proposed by Arslan [4] is based on endmembers extraction using Pixel Purity Index (PPI) and the n-D Visualizer (ENVI® tools). But it is not an automatic method and some degree of subjectivity exists in extracting endmembers.

The advantage of the methods proposed in this paper is that they can detect hydrocarbon pollution, without knowing a priori the type of hydrocarbon that has spilled, with an automatic processing.

2. MATERIAL AND METHODS

The data studied is an AVIRIS image acquired above Bay Jimmy, south of New Orleans on September 14, 2010, and located between 29.252639°N, 89.907328°W and 29.588961°N, 89.859397°W. Available image are geo-corrected with a 3.5 m spatial sampling. Data are in radiance unit with 224 contiguous spectral bands from 400 to 2500 nm and a spectral sampling of 10 nm. In this work a part of this image shown in Figure 1 is processed.

2.1. Pre-processing

Before applying oil detection, some pre-processing is needed. First of all, the image is converted in reflectance unit using the atmospheric correction software COCHISE [6], that compensated the effects of atmospheric scattering and molecular absorption, in particular water vapor absorption. Radiative transfer parameters are calculated via MODTRAN 5.3 (MODerate resolution atmospheric TRANsmission) [7]. Past this stage, 196 spectral bands among the 224 are retained because some large and strong water vapor absorption bands are removed as well as some noisyl bands near 2.5 µm.

In order to denoise the data, a Minimum Noise Fraction transformation is applied. Components that correspond to noise are ignored when applying the reverse MNF to reconstruct the image.

Figure 1: RGV extract of AVIRIS image over Bay Jimmy.

2.2. Automatic mapping based on hydrocarbon indices

The first method, which has been developed, uses a new hydrocarbon index to directly detect the oiled areas.

As a matter of fact, the spectral signature of hydrocarbons is characterized by two absorption bands (denoted as AB), the first at about 1.73 µm (C-H stretch of the first overtone band) and the second at 2.31 µm (C-H stretch combination band). The 1.73 µm AB is much specific to hydrocarbon but senescent vegetation can be confused with oil in this spectral range. The potential of the 1.73 µm AB for hydrocarbon detection has been demonstrated in [8]. Kühn et al. [9] defined a spectral Hydrocarbon (denoted as HC) Index, which is the depth of the 1.73 µm AB. This index allowed detection of soil-hydrocarbon mixtures as well as plastic materials. In the present case, this index failed to detect the polluted coasts.

We defined a new hydrocarbon index, Area1700, that calculates the area of the absorption features under a virtual line drawn between λ_a=1.658 and λ_b=1.754 µm (Figure 2). The advantage of this index is that it is less sensitive to noise and to the position of the center of the AB that can varies with the hydrocarbon composition.

This index is applied on the image as shown on Figure 3. This allows mapping oiled coastal lines, but it also detects materials that contain hydrocarbon, such as boats, because of plastic component that have very high HC score. Buoys that were deployed to prevent oil to reach the coasts are also detected, but with a lower HC score than oiled coast, due to their small size. The histogram of HC scores image presented in Figure 3 is adjusted on a part of the image containing no boats, because their high HC scores flatten the scale of HC scores of oiled coast lines.

The Kühn index is also depicted on Figure 3. It does not detect all the oiled shorelines and is very sensitive to noise.

The detection map thus obtained is in good agreement with results of previous works carried out on the same area at the same day [3] (see Figure 4). It is also compared with the map drawn from ground observations three days after, on September 17th, 2010 available in the Environmental Response Management Application (ERMA) website [10] (see Figure 5). The oiled soils detected with Area 1700 are quite similar to the most impacted soils depicted in red and orange. Some false alarms are present in the in-land vegetation.

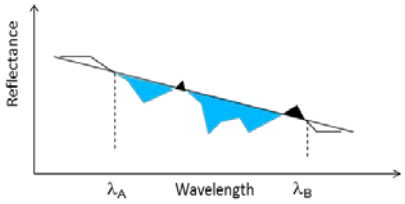

Figure 2: Area1700 index. To calculate Area1700 index, only the blue parts are counted.

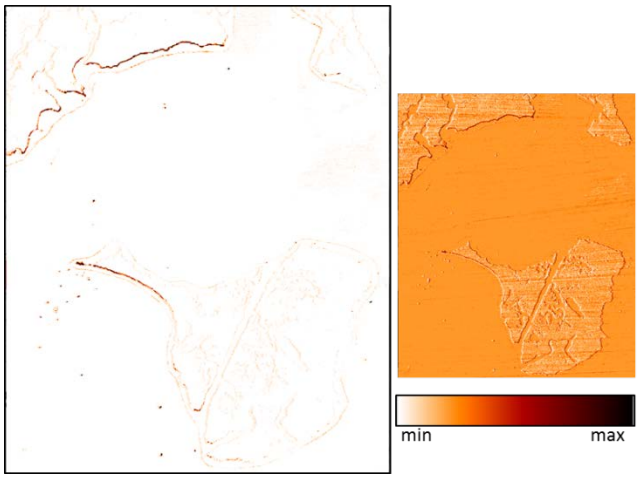

Figure 3: Area 1700 HC and Kuhn HC indices. Histograms have been ajusted on a part of image containing no boat.

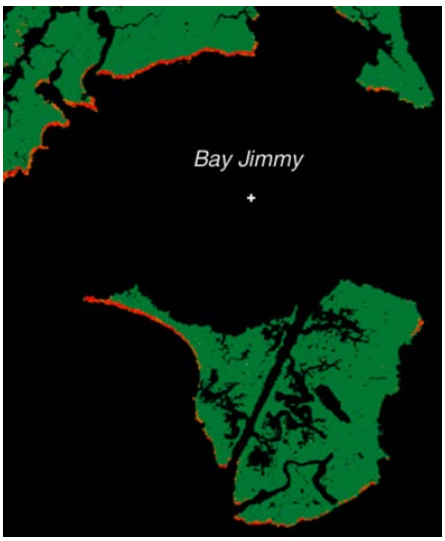

Figure 4 – Oiled coastlines mapped by Kokaly for the same Aviris image (2013).

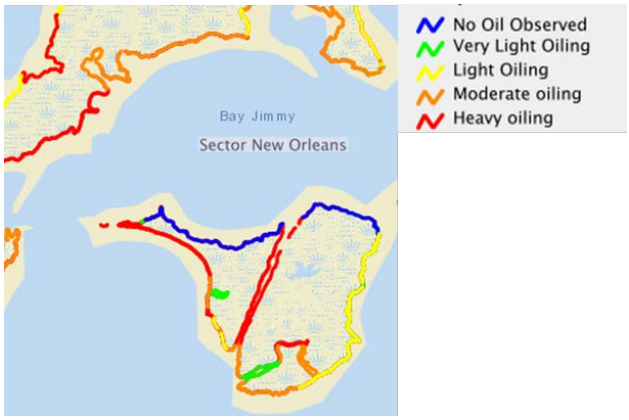

Figure 5 : ERMA, September 17, 2010 – SCAT (Shoreline Cleanup and Assessment Technique) oiling ground observations.

2.3. Automatic mapping with endmembers extraction

The second method we developed is based on endmembers extraction and linear unmixing, which is a classic approach to identify pure materials in a hyperspectral image and to calculate their related abundances in each pixel. The assumption is done that the different pure components (endmembers) are linearly mixed in the pixels. Such problem can be formulated as follows:

$$p_{ij} = \sum_{k=1}^{K} e_{ik} a_{kj} + w_{ij} \quad s.t. \quad 0 \leq a_{kj} \leq 1 \;\&\; \sum_{k=1}^{K} a_{kj} = 1$$

where p_{ij} is the radiance or the reflectance of the pixel j in the band i, and e_{ik} is the radiance (or reflectance) of the endmember k in the band i, and a_{kj} is the abundance of the endmember k in the pixel j.

In order to avoid the detection of numerous undesirable elements during the endmembers extraction, a mask was applied to the boats, as well as to the plastic buoys surrounding the islands, when using this approach. To extract endmembers, a method based on the Orthogonal Subspace Projection (OSP) is used [11]. We chose OSP because it is very simple to implement and its results are reproducible, as the method does not use any random draw. More, it is not necessary to know the real number of endmembers, whose determination is a complex issue and has strong impact on the results of most of the endmembers extraction methods. In OSP, increasing the number of endmembers do not change the endmembers already extracted. In this work, this number was set to 20. The principle of this method is to search iteratively for extrema pixels. At each iteration data are projected orthogonally to the subspace supported by the endmembers previously extracted. Endmembers extraction is applied on a spectral subset which only contains specific HC spectral features. The bands 119 to 140 and 143 to 196 are kept, that correspond to the spectral ranges 1.5923 µm - 1.8015 µm and 1.9674 µm - 2.4962 µm. After the endmembers extraction, abundances map of each endmembers are computed using FCLS (Fully Constrained Least Squares) method. The next stage consists in finding the endmembers of interest, i.e. corresponding to the oil impacted materials. To do so, endmembers are sorted in descending order according to their HC scores. Two HC indices are considered Area1700 and Area2300, which is the area of the absorption features under a virtual line drawn between λ_a=2.21 µm and λ_b=2.38 µm, computed in the same way as Area1700. For more clarity, hydrocarbon indices have been normalized. The Table 1 presents the sorted endmembers according to their HC indices (number in parentheses). It shows that the 3rd, then the 5th endmembers are the best as they have high scores for both normalized indices.

The figure 6 shows the spectrum of the endmembers 3, 5, 14 and 17 that appear in Table 1. The absorption bands at 1.72 and 2.3 µm are clearly observable.

Table 1 – Endmembers sorted according to their normalized HC scores Area1700 and Area2300 (in parentheses).

	Area1700	Area2300
1	3rd (1.000)	3rd (1.000)
2	14th (0.665)	5th (0.680)
3	5th (0.487)	17th (0.517)

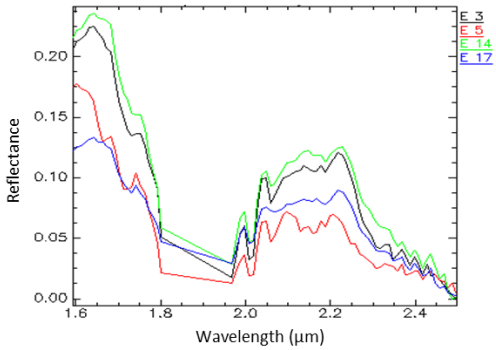

Figure 6 – Endmembers spectra.

The abundance maps corresponding to the 3rd endmember and to the sum of the 3rd and the 5th endmembers are shown on Figure 7. They can be compared to Figure 4 and Figure 5. The detected oiled areas are similar to those obtained by Kokaly [3] and with the high and moderate oiled areas observed on the field three days after [10]. The sum of the 3rd and 5th endmembers abundances map enhanced a little more the oiled areas. The abundance maps of endmembers 14 and 17 (not shown in this paper) allow identifying parts, but not all, of oiled shorelines.

Finally, this method based on linear unmixing gives similar results as those based solely on HC index calculation, with slightly fewer false alarms on in-land vegetation.

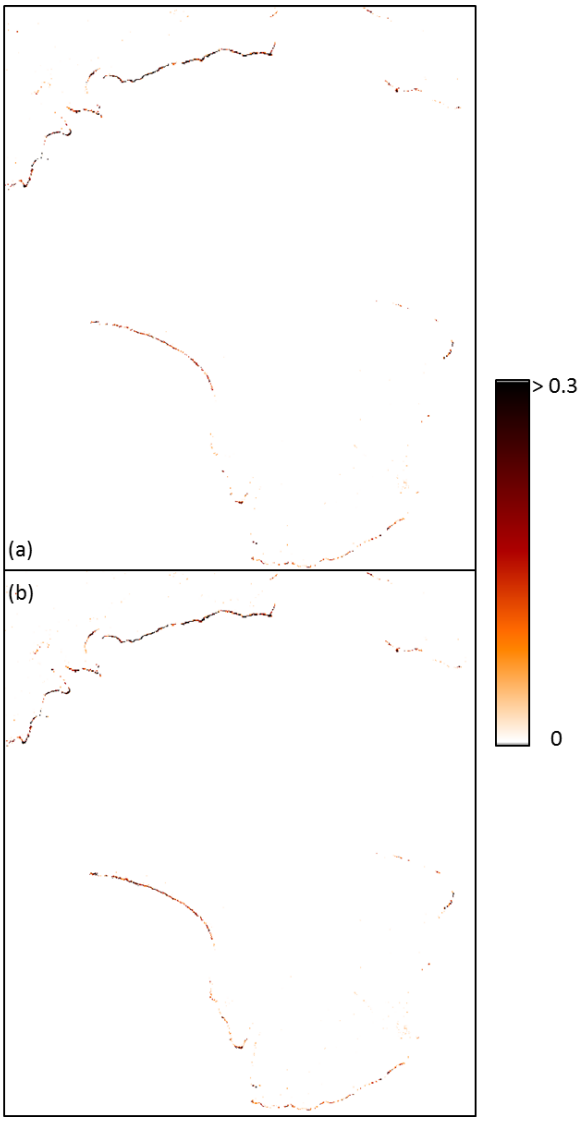

Figure 7: Abundance of the 3rd endmember (a) and sum of the abundances of the 3rd and 5th endmembers (b). Histograms are adjusted on the whole images.

3. CONCLUSION

Both technics presented in this paper allow the detection of oil spilling on shoreline. They make it possible to detect oiled coastline with very few false alarms, even in presence of senescent plants that are known to cause false alarms when detecting oiled materials using the 1.73 µm absorption band. The detected areas are consistent with field observations [1] and with those obtained in [3] and [4]. In addition, compared with these previous works, the proposed methods have the advantage of not requiring fields or lab measurements and of being fully automatic. The first method is very simple to implement because it only requires the calculation of a new HC index, Area1700, which is presented in this paper. This new HC index is significantly more efficient for detecting polluted coastlines than the index proposed by Kühn and using the same absorption band. The second method developed in this work is based on endmember extraction and linear unmixing. Endmembers that are used to map oiled shorelines are selected according to their Aire1700 and Aire2300 scores. This method, has a little more complex implementation, but gives significantly better results that the first one. But in order to limit to number of useless endmembers, a mask has been built to hide boats and buoys, which requires a manual pre-processing.

4. REFERENCES

[1] United States Coast Guard, and U.S National Response Team. On scene coordinator report: Deepwater Horizon oil spill, Geological Survey open-file report, 2011

[2] Kokaly, R. F, D. Heckman, J. Holloway, S. Piazza, B. Couvillion, G. D. Steyer, C. Mills and T. M. Hoefen, Shoreline surveys of oil-impacted marsh in southern Louisiana. U.S, U.S. Geological Survey Open-File Report 2011–1022, 2011

[3] Kokaly, R. F., B. R. Couvillion, J. A. M. Holloway, D. A. Roberts, S. L. Ustin, S. H. Peterson, S. Khanna, S.C. Piazza, Spectroscopic remote sensing of the distribution and persistence of oil from the Deepwater Horizon spill in Barataria Bay marshes. Remote Sensing of Environment, 129, 210-230, 2013

[4] Arslan, M. D, Oil Spill Detection and Mapping Along the Gulf of Mexico Coastline Based on Imaging Spectrometer Data. Texas: Texas A & M University PhD report, 2013

[5] Kokaly, R. F., Spectroscopic remote sensing for material identification, vegetation characterization, and mapping, Proc. SPIE, Vol. 8390, 839014, doi: 10.1117/12.979120, 2012

[6] Miesch, C. P., Poutier, L.; Achard, V.; Briottet, X.; Lenot, X.; Boucher Direct and inverse radiative transfer solutions for visible and near-infrared hyperspectral imagery. IEEE Trans. Geosc. Remote Sensing, vol. 43, n°7, 1552-1562, 2005

[7] Berk A., et al, MODTRAN5: a reformulated atmospheric band model with auxiliary species and practical multiple scattering options, Proc. SPIE, Vol. 5571, p. 78-85 doi: 10.1117/12.564634, 2004

[8] Hörig, B., Kuhn, F.; Oschutz, F.; Lehmann, F., HyMap hyperspectral remote sensing to detect hydrocarbons. Int. Journal of Remote Sensing, 1413-1422, 2001

[9] Kühn, F., Oppermann, K. and Horig, B., Hydrocarbon Index - An algorithm for hyperspectral detection of hydrocarbons, Int. Journal. of Remote Sensing.. 25, 2467-2473., 2004

[10] https://erma.noaa.gov/gulfofmexico/erma.html

[11] Chang, C.-I., Orthogonal subspace projection (OSP) revisited: a comprehensive study and analysis. IEEE Trans. on Geoscience and Remote Sensing, Vol. 43, no. 3, 502-518, 2005